Adoptive transfer of mitochondrial antigen-specific CD8$^+$ T-cells in mice causes parkinsonism and compromises the dopamine system.

Elemeery MN[1-2-3-4-5-6-7], Tchung A[1-2-3-4], Boulet S[5-7], Mukherjee S[1-2-3-4-5], Giguère N[1-2-3-4-5], Daudelin J-F[5-7], Even A[1-2-3-4-5], Hétu-Arbour R[5-7-8], Matheoud D[2, 9], Stratton JA[5,10], Labrecque N[5-7-8-9-11-12]*, Trudeau L-E[1-2-3-4-5]*

*Co-corresponding authors

[1]Department of pharmacology and physiology, Faculty of Medicine, Université de Montréal
[2]Department of neurosciences, Faculty of Medicine, Université de Montréal
[3]Neural Signaling and Circuitry research group (SNC)
[4]Center for Interdisciplinary Research on the Brain and Learning (CIRCA)
[5]Aligning Science Across Parkinson's (ASAP) Collaborative Research Network, Chevy Chase, MD, USA, 20815.
[6]Medical Biotechnology Department, National Research Centre, Dokki, Giza, Egypt
[7]Centre de recherche de l'hôpital Maisonneuve-Rosemont (CRHMR)
[8]Institut de recherches cliniques de Montréal (IRCM)
[9]Centre de recherche du Centre hospitalier universitaire de l'Université de Montréal (CRCHUM)
[10]Dept. of Neuroscience and Neurology, Montreal Neurological Institute-Hospital, McGill University, Montreal,
[11]Department of medicine, Faculty of Medicine, Université de Montréal
[12]Department of microbiology, infectious diseases and immunology, Faculty of Medicine, Université de Montréal

Running Title: Mitochondrial peptide-specific T cells and Parkinson's disease.

Corresponding authors:
Dr. Louis-Éric Trudeau
Department of pharmacology and physiology
Faculty of Medicine
Université de Montréal
louis-eric.trudeau@umontreal.ca
514-343-5692

Dr. Nathalie Labrecque
Institut de recherches cliniques de Montréal
Department of medicine
Faculty of medicine
Université de Montréal
nathalie.labrecque@umontreal.ca
514-987-5502

Abstract

The progressive dysfunction and degeneration of dopamine (DA) neurons of the ventral midbrain is linked to the development of motor symptoms in Parkinson's disease (PD). Multiple lines of evidence suggest the implication of neuroinflammation and mitochondrial dysfunction as key drivers of neurodegenerative mechanisms in PD. Recent work has revealed that loss of the mitochondrial kinase PINK1 leads to enhanced mitochondrial antigen presentation (MitAP) by antigen-presenting cells (APCs), the amplification of mitochondrial antigen-specific $CD8^+$ T cells and the loss of DA neuron terminals markers in the brain in response to gut infection. However, whether mitochondrial antigen-specific T cells are involved in and/or sufficient to cause DA system dysfunction remains unclear. Here, we investigated the effect of mitochondrial autoimmunity by adoptively transferring mitochondrial peptide-specific $CD8^+$ T cells into wild-type (WT) and PINK1 KO mice. We find that this leads to L-DOPA-reversible motor impairment and to robust loss of DA neurons and axonal markers in the striatum in both PINK1 WT and KO mice. Our findings provide direct evidence of the pivotal role played by mitochondrial-specific $CD8^+$ T cell infiltration in the brain in driving PD-like pathology and the development of parkinsonism. Altogether, our data strongly support the hypothesis that MitAP and autoimmune mechanisms play a key role in the pathophysiological processes leading to PD.

Key words: Parkinson’s, lymphocytes, dopamine, mitochondria, immune, PINK1

Introduction

The motor symptoms of Parkinson's disease (PD), including bradykinesia, akinesia, rigidity and tremors, are caused in part by the progressive degeneration of substantia nigra pars compacta (SNc) dopamine (DA) neurons, leading to loss of DA in the striatum and dysregulation of basal ganglia circuits that regulate movement initiation. Disease modifying therapies are not presently available and current therapeutic strategies such as L-DOPA or DA receptor agonists focus on alleviating symptoms by partially restoring basal ganglia circuit function. A growing literature emerging from the study of the genes linked to familial, genetic forms of PD, suggests that the functions of ubiquitous cellular compartments such as mitochondria, lysosomes and vesicles are compromised by the loss of function of proteins such as PINK1 or Parkin [1-5] found in mitochondria or LRRK2 and GBA [6-9], found in lysosomes. Cellular dysfunctions could thus happen in multiple cell types and not only in neurons.

Cells of the immune system and inflammatory mechanisms are increasingly considered as playing a role in the initiation or progression of PD. Notably, increased levels of cytokines such as IL-1β, TNF-α, IFN-γ and IL-6 have been reported in the cerebrospinal fluid and nigrostriatal regions of PD subjects relative to age-matched controls [10, 11]. The presence of T cells in the brain of PD subjects has also been reported [12] as well as the presence in the blood of antibodies and T cells recognizing alpha-synuclein antigens [13-15]. Entry of $CD4^+$ T cells in the brain of a PD mouse model overexpressing alpha-synuclein has also been reported [16, 17], and increased brain inflammation and neuronal loss has been found in rats overexpressing alpha-synuclein [18]. Loss of function of PINK1 or Parkin was discovered to lead to disinhibition of mitochondrial antigen presentation (MitAP) in antigen presenting cells (APCs) [1]. Furthermore, in PINK1 KO mice, a gastrointestinal infection was shown to lead to the amplification of mitochondrial antigen-specific $CD8^+$ T cells, to loss of DA neuron terminals

markers in the striatum and to impaired motor functions [19]. Together, this work raises the possibility that autoantigens and autoimmune mechanisms are involved in PD [20-22], a conclusion also supported by recent work on LRRK2 [23].

However, whether mitochondrial antigen-specific T cells are sufficient to cause DA system dysfunction remains undetermined and a critical question to tackle. To address this possibility, here we took advantage of 2C transgenic mice that express a T cell receptor (TCR) specific for a mitochondrial antigen derived from 2-oxoglutarate dehydrogenase (OGDH) [24, 25]. We tested the hypothesis that peripheral adoptive transfer of activated $CD8^+$ T cells from 2C mice in PINK1 KO mice would lead to an attack of the DA system in the brain of these mice. Compatible with this hypothesis, we find that this leads to L-DOPA reversible motor impairment and to robust loss of DA neurons and axonal markers in the striatum in both PINK1 WT and KO mice. This work establishes a new mouse model that could be critical to identify the mechanisms whereby mitochondrial antigen-specific $CD8^+$ T cells interact with DA neurons and other vulnerable neurons, leading to brain pathology in PD.

Materials and methods

Mice. 2C[24, 25], OT-I[26] and Pink1 KO mice (Jackson Laboratory, Strain #017946) and wild type (WT) littermate controls were maintained in rigorous adherence to the principles of good animal practice as defined by the Canadian Council on Animal care and according to protocols approved by the animal ethics committee (CDEA) of the Université de Montréal and of the Research Center of the Maisonneuve-Rosemont Hospital.

T cell purification and activation. Naïve $CD8^+$ T cells from the spleen of 2C and OT-I TCR transgenic mice were purified using a Easysep™ Mouse naïve $CD8^+$ purification kit (STEMCELL, BC, Canada). Purified naïve $CD8^+$ T cells were then activated using anti-CD3/CD28 stimulation. Briefly, 24-wells plates were coated with 1 µg/ml of anti-CD3 antibody (BioXcell, clone 14-2C11; Cat # BE0001-1) diluted in sterile PBS and then incubated at 5% CO2 at 37°C for 2h. 10^6 naïve $CD8^+$ T cells were seeded on CD3-coated wells and anti-CD28 antibody (BioXcell, clone 37-51; cat # BE0015-1) was added to reach a final concentration of 5 µg/ml. Cells were stimulated for 72h at 37°C before harvesting for adoptive transfer. The proper activation of $CD8^+$ T cells was validated by measuring the up-regulation of CD44, CD25 and CD69 and down-regulation of CD62L by flow cytometry.

Adoptive transfer of TCR transgenic T cells. Pink1 KO and WT littermate control mice were injected i.p with 5 X 10^6 activated 2C or OT-I $CD8^+$ T cells diluted in 200 µl of sterile PBS. Some control mice were not injected with T cells. 48h after adoptive transfer, all mice were treated with pertussis toxin (PTx) (i,p 20ug/kg; Cayman chemical, cat# 23221) to facilitate T cell infiltration in the brain.

FACS analysis. 200 µl blood samples were collected in PBS containing 2mM EDTA from jugular vein at both early (day 7) and late (day 40) time points after the adoptive transfer. Spleens were also collected at day 7 for some mice and from all the mice at end point. Red blood cells were lysed using NH4CL 0.86% before staining. Samples were stained first with the Zombie NIR viability dye (1:1,000) for 20 min at 37°C, then with anti-CD16/CD32 for 20 min at 37°C followed by staining with antibodies directed against different cell surface markers for 20 min at 4°C. To track OT-I cells, K^b-OVA tetramer (NIH Tetramer core facility) staining was done at 37°C for 15min. Samples were analyzed using the BD LSRFortessa X-20. The antibodies used for flow cytometry are listed in **Table 1**.

Table 1: List of antibodies used for flow cytometry.

Antibody		**Supplier**	**Product information**
1B2	Biotin	Custom made	F23.1, 53-6.72 (rat anti-mouse CD8).
CD101	PE-Cy7	ThermoFisher	Clone Moushi101; cat # 25-1011-80
CD11b	BV711	Biolegend	Clone M1/70; cat # 101242
CD127	BV421	Biolegend	Clone A7R34, cat # 135027
CD25	APC	Biolegend	Clone PC61; cat # 102012
CD4	BV605	Biolegend	Clone RM4-5; cat # 100548
CD44	APC-cy7	Biolegend	Clone IM7; cat # 103028
CD45.2	FITC	Biolegend	Clone 104; cat # 110706
CD45.2	Alexa flour 700	Biolegend	Clone 104; cat # 109822
CD62L	PercP	Biolegend	Clone MEL; cat # 104430
CD69	APC	Biolegend	Clone H1.2F3; cat # 104513
CD8	BV785	Biolegend	Clone 53-6.7; cat # 100750
CXCR3	PE	Biolegend	Clone CXCR3-173; cat # 126505
CXCR6	PEdazzle594	Biolegend	Clone SA051D1; cat # 151116
KLRG1	APC	Biolegend	Clone 1MAFA; cat # 138412
P2XR7	PercP-Cy5.5	Biolegend	Clone 1F11; cat # 148710
K^b-$OVA_{257-264}$		NIH Tetramer core facility	

Isolation of brain infiltrating lymphocytes. To discriminate the T cells that have infiltrated the brain from the ones circulating in the blood, mice were injected i.v. with anti-CD45-FITC (BD) and sacrificed 3-5 min later for brain collection. The T cells that have infiltrated the brain are protected from this short staining and as such, will be CD45-FITC negative in the flow cytometry analysis. To dissociate the brain, the tissue was minced using a scalpel longitudinally to not less than 8 pieces and digested in RPMI containing 0.01 mg/ml DNase I and 0.5 mg/ml collagenase D for 40 min using the gentleMACS Octo dissociator at 37°C before filtration through a 70μm filter. To isolate lymphocytes, samples were centrifuged, resuspended in 3 ml of 37% Percoll solution diluted in RPMI, layered over another 3 ml of 70% Percoll, and centrifuged at 2000 r.p.m. without brake at 25 °C for 20min to collect the buffy coat leukocytes interlayer.

Immunohistochemistry. To prepare brain sections, PINK1 KO and WT littermate mice were deeply anaesthetized with pentobarbital (70 ug g^{-1}, i.p.) before intracardiac perfusion with 50ml cold PBS (0.01 M) followed by 50ml of cold 4% paraformaldehyde (PFA). Then, the brain was collected, post-fixed for 24h in PFA solution at 4°C, followed 30% sucrose solution (5.382g/l sodium phosphate monobasic, 8.662g/l sodium phosphate dibasic anhydrous, and 300g/l sucrose, dissolved in distilled water) for 48h. Serial coronal (40μm thickness) free-floating sections were cut using a Leica CM1950 cryostat and collected in an antifreeze solution (1.57g/l sodium phosphate monobasic anhydrous, 5.45g/l sodium phosphate dibasic anhydrous, 300ml ethylene glycol, 300ml glycerol, dissolved in distilled water). Coronal sections underwent permeabilization using Triton X-100 (0.1%), after which nonspecific binding sites were blocked by incubating in bovine serum albumin (100 mg/ml) (0.02% NaN3, 0.3% Triton X-100, 10% BSA, and 5% serum of the same host used for the secondary antibody). Sections then underwent permeabilization using a Triton X-100 (0.1%) based solution (0.02% NaN3, 0.1% Triton

X-100, 0.5% BSA, and 5% serum). The sections were subsequently incubated overnight with a rabbit anti-TH antibody (1:2000, AB152, Millipore Sigma, USA), a rat anti-DAT antibody (1:2000, MAB369; MilliporeSigma, USA), rabbit anti-Sert antibody (1:2000, PC177L-100UL, Sigma, USA) or mouse anti-NeuN antibody (1:1000, Abcam, USA) as well as DAPI to label nuclei (1:2000, D9542, Sigma Aldrich, USA). Quantitative analyses of fluorescence imaging on brain slices were conducted using images acquired through a Nikon AX-R automated point-scanning confocal microscope (Nikon NY, U.S.A). Images (2048x2048 px resolution, Nyquist, galvanometer scanning mode with 1x averaging and 0.8ms dwell time) were captured using PLAN APO AD 40× OFN25 DIC N2 objective lens (0.6 NA**,** Nikon Canada) from dorsal and ventral striatum fields. The dorsal striatum encompassed the compartment superior to the anterior commissure and inferior to the corpus callosum, while the ventral striatum included the nucleus accumbens shell and core. In the dorsal striatum, image acquisition involved selecting four random fields on each side from both hemispheres in each section. In the ventral striatum, two fields per hemisphere were chosen in each section. Image quantification, performed using FIJI (National Institutes of Health) software, entailed applying a uniform threshold to all analyzed images after determining the average background signal intensity, which was then subtracted from the raw images. The quantification of TH+ and SERT+ axon terminals in dorsal striatal sections involved averaging eight fields per section, with eight independent sections quantified for each mouse. In the ventral striatum sections, the analysis averaged four fields per section, and five independent sections were quantified for each mouse.

Stereological analysis. Brain sections were rinsed in 0.01 M PBS for 10min before immersion in 0.01 M PBS with 0.9% H_2O_2 for another 10min. The sections were then rinsed three times in 0.01 M PBS after which they were incubated with rabbit anti-TH antibody at a 1:1000 dilution in a solution

containing 0.3% Triton X-100, 50 mg/ml BSA, and 0.01 M PBS, for 48h at 4°C. This was followed by further rinses in 0.01 M PBS (3 × 10min) and a 12h incubation at 4 °C in biotin-streptavidin conjugated AffiniPure IgG (anti-rabbit-streptavidin Jackson Immunoresearch, 1:200), followed by three washes with 0.01 M PBS. Subsequently, sections were incubated for 3h at room temperature in streptavidin horseradish peroxidase (HRP) conjugate (GE Healthcare, 1:200) diluted in 0.3% Triton X-100 in 0.01 M PBS. Visualization was achieved through a 5min 3,3′-diaminobenzidine tetrahydrochloride (Sigma-Aldrich)/glucose oxidase reaction, after which sections were mounted on charged microscope slides in 0.1 M acetate buffer, counterstained with cresyl violet, defatted via a series of ethanol and xylene baths, and finally coverslipped using permount (Fisher Scientific. Cat # SP15-100). The quantification of the number of TH neurons in both the substantia nigra pars compacta (SNc) and ventral tegmental area (VTA) employed unbiased stereological counting methods. The total number of TH neurons was determined using the optical fractionator method [27] with Stereo Investigator (version 6; MicroBrightField). Briefly, TH-immunoreactive neurons were counted in every sixth section at 100× magnification using a 60 × 60-µm2 counting frame. A 10µm optical dissector with two 1µm guard zones was utilized, and counting sites were positioned at 100µm intervals following a random start. A minimum number of 6 brain sections from each mouse including the SNc was used as an inclusion criterion.

Behavioral tests. All behavioral experiments were performed during the night cycle (active phase for mice), on both female and male mice of both genotypes. The investigator was blinded to both genotype and the treatment group during experimental procedures. To reduce the stress introduced by the examiner on the mice, mice were allowed to habituate to the examiner for not less than 5min per mice for 3 to 5 successive days. Mice housed at 2-4 mice in a cage were then tested at 42 to 52 days after the

adoptive transfer. On the test day, mice were transferred to the testing room and allowed a resting time of 60min before testing.

Basal locomotor activity. Open field automated activity chambers (Superflex, Omnitech, U.S.A) were used to quantify horizontal activity and vertical episode counts. All experiments were performed at the same time of the day using mice maintained on a 12h light/dark cycle from 22:00 to 10:00. Mice were placed individually in activity boxes (41 × 41 cm) and their horizontal and vertical activity were measured by quantifying photocell beam breaks. Data were analyzed by the fusion software version 5.3 (Omnitech, Ohio, U.S.A).

Grip strength test. Grip strength tests were performed with a grip strength meter (BioSeb, France, model Bio-GS3). Mice were tested three times, and the results were averaged for each mouse. The muscular strength of mice was quantified by measuring the force needed (g) to remove the four paws from the grid. Each mouse was weighed before the grip strength test. Results are expressed as gram-force normalized to body weight.

Pole test. The pole utilized in this experiment was a 60cm metal rod with a diameter of 10mm. The rod was covered with adhesive tape to enhance traction and securely positioned within a housing cage. Mice were oriented head-up at the top of the pole, and the time taken for both turning and to complete descent was meticulously recorded. Treatment groups received either 6.5 mg/kg of benserazide (Sigma, B7283) combined with 25 mg/kg of l-DOPA (Sigma, D1507), or an equivalent volume of saline. Mice that did not descend from the pole after 180s were considered to have failed the test, returned to their home cage and re-tested later.

Results

Mitochondrial peptide-specific CD8$^+$ T cells infiltrate the brain and are found in higher numbers in PINK1 KO mice.

We tested the hypothesis that mitochondrial peptide-specific CD8$^+$ T-cells can induce PD-like pathology and parkinsonism in mice following their adoptive transfer into PINK1 KO mice. To do so, we adoptively transferred 5 X 10^6 *in vitro* activated CD8$^+$ T cells from 2C TCR transgenic mice, which express a TCR specific for the mitochondrial antigen OGDH, into PINK1 WT or KO mice (**Fig. 1a**). As a control, PINK1 WT and KO mice were adoptively transferred with activated CD8$^+$ T cells from OT-I TCR transgenic mice expressing a TCR specific for the ovalbumin antigen. Forty-eight hours after adoptive transfer, pertussis toxin (20 µg/kg) was administered i.p. to facilitate brain infiltration of the transferred CD8$^+$ T cells. Blood samples were collected at day 7 or 40 after the adoptive transfer to assess the persistence and abundance of the transferred cells. The transferred cells were tracked using either a monoclonal antibody (1B2) specific for the TCR expressed by the 2C CD8$^+$ T cells or with the K^b-OVA tetramer for control OT-I CD8$^+$ T cells. The gating strategy in described in **Supplemental Fig. 1**. We were able to detect the transferred 2C and OT-I CD8+ T cells in the blood of the recipient mice both at 7 and 40 days after the adoptive transfer, with a higher frequency of the 2C compared to the OT-I CD8$^+$ T cells (**Fig. 1b-c)**. Although the proportion of 2C CD8$^+$ T cells in the blood of the transferred mice was not significantly different between PINK1 KO and WT mice (**Fig. 1b-c**), the absolute number of such cells detected in the spleen at day 40 was higher in the PINK1 KO mice compared to WT littermates (**Fig. 1d and Supplementary Fig.1**). Altogether, these observations indicate that mitochondrial peptide-specific 2C CD8$^+$ T-cells accumulate more than OT-I CD8$^+$ T cells in PINK1 KO and WT mice suggesting that 2C T cells encounter their antigen in recipient mice. Moreover, as more

2C $CD8^+$ T cells were recovered in PINK1 KO mice compared to PINK1 WT recipients, these findings suggest that they may have seen more mitochondrial antigens in PINK1 KO mice.

We then asked whether the adoptively transferred 2C $CD8^+$ T cells were infiltrating the brain of the recipient mice. Seven or 40 days after the adoptive T cell transfer, FITC-labelled anti-CD45 antibodies were injected i.v. 3-5 min prior to brain collection. This allows to label circulating lymphocytes and distinguish them from those that had entered in the brain (**Supplementary Fig. 1**). We found that both 2C and OT-I $CD8^+$ T cells infiltrated the brain and were readily detectable at both 7 and 40 days after the adoptive transfer, with an increased abundance at day 40 (**Fig. 1e-f**). The absolute number of 2C $CD8^+$ T cells was higher in PINK1 KO mice compared to WT control mice (**Fig. 1e-f**). The results demonstrate that mitochondrial antigen-specific $CD8^+$ T-cells infiltrate and accumulate in the brain, and this is enhanced in the absence of functional PINK1 protein in the recipient mice.

Figure 1

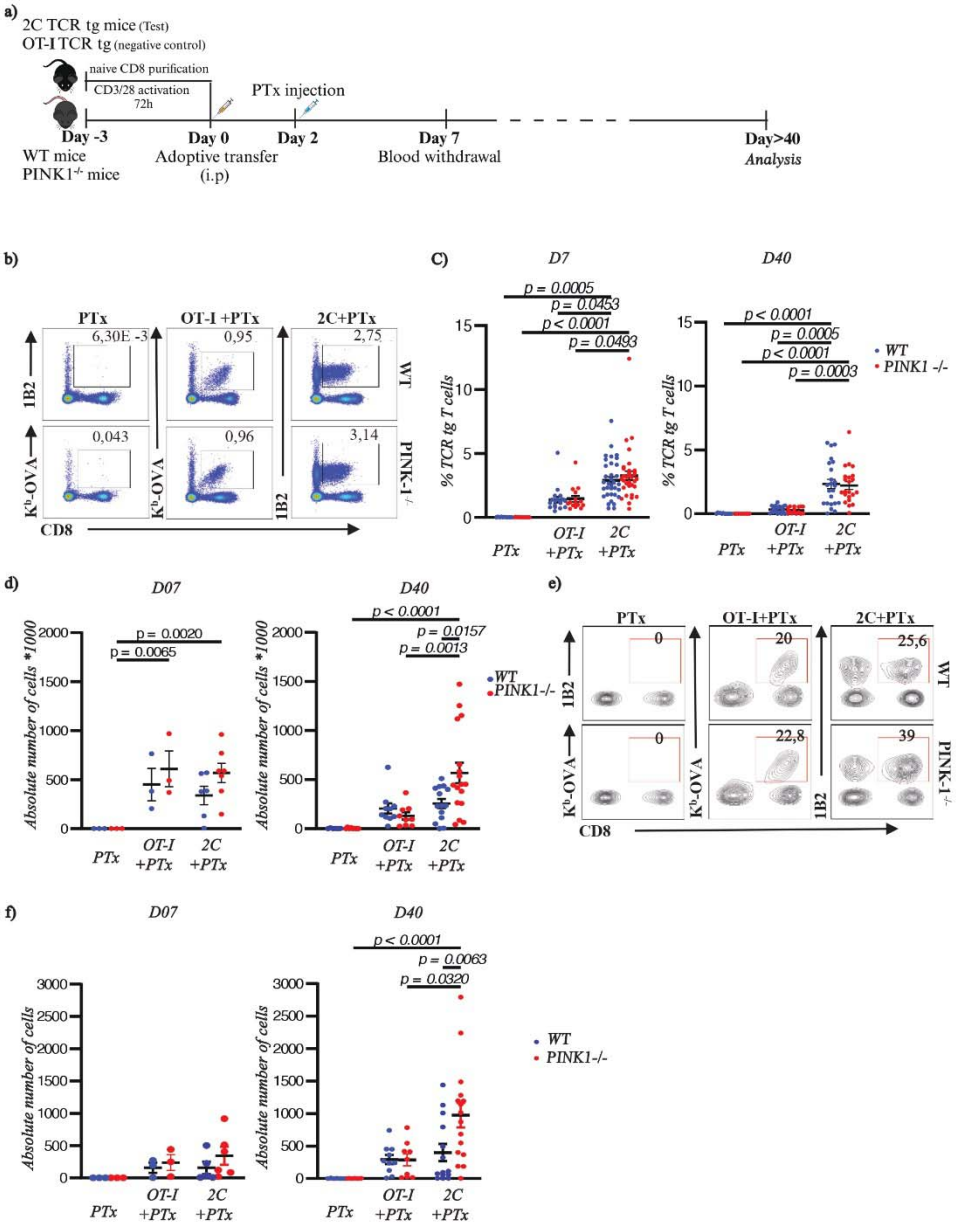

Figure 1: Adoptively transferred mitochondrial antigen-specific CD8$^+$ T cells persist in the circulation and infiltrate the brain in higher amounts in PINK1 KO mice. a) Schematic diagram outlining the experimental workflow. **b)** Representative flow cytometry profiles for the detection of adoptively transfer TCR transgenic CD8$^+$ T cells. 2C T cells were identified using the anti-TCR clonotype antibody 1B2 (CD8+1B2+) while OT-I T cells were identified using K^b-OVA tetramer staining (CD8+Kb-OVA+). PTx refers to mice that were not adoptively transferred and only received the Ptx treatment. **c)** Frequency of the adoptively transferred TCR transgenic CD8$^+$ T cells in the blood at day 7 and 40 after the adoptive transfer in WT and PINK1 KO mice. **d)** Absolute number of adoptively transferred TCR transgenic CD8$^+$ T cells in the spleen of WT and PINK1 KO mice. **e)** Representative flow cytometry profiles for the detection of adoptively transfer TCR transgenic CD8$^+$ T cells that have infiltrated into the brain. **f)** Absolute number of adoptively transferred TCR transgenic CD8+ T cells that infiltrated the brain of WT and PINK1 KO mice at 7 days (left) and 40 days (right) after the

adoptive transfer. Each dot represents the results obtained from one mouse. Data is representative of a minimum of three independent experiments. p values were determined using two-way ANOVA followed by Tukey's multiple comparisons post-hoc test. Data are presented as mean ± s.e.m. Data from male and female mice were pooled.

Adoptive transfer of mitochondrial antigen-specific CD8$^+$ T cells leads to L-DOPA reversible motor impairment in both PINK1 KO and WT mice.

Our observation of entry of the adoptively transferred CD8$^+$ T cells in the brain raised the possibility that mitochondrial antigen-specific 2C CD8$^+$ T cells could recognize their antigen in the brain, leading to DA neuron loss and motor circuit dysfunction. Compatible with this hypothesis, we observed that after a period of 30 days or more following the adoptive transfer, some of the mice showed impaired locomotion in their home cages following qualitative observations. To validate this, we performed more extensive behavioral phenotyping using open field locomotor analysis, grip strength analysis, a rotarod task and the pole test. In the open field, we found reduced movement distance and vertical episodes in the mice transferred with 2C CD8$^+$ T cells, but not in the mice transferred with OT-I CD8$^+$ T cells or only injected with Ptx (**Fig. 2a-b**). Similar effects were seen in PINK1 KO and WT recipients. The time spent in the center of the open field, often used as an indirect index of anxiety, was not altered (**Fig. 2c**). No differences were observed in the grip strength test (**Fig. 2d**). In the rotarod task, the maximal speed leading to falling off the apparatus and the time to fall was lower in the mice that had undergone 2C CD8$^+$ T cell adoptive transfer compared to the other groups (**Fig. 2e**), with here again the genotype of the recipient mice having no impact. Finally, in the pole test, the mice transferred with 2C CD8$^+$ T cells, but not the mice transferred with OT-I CD8$^+$ T cells or treated only with PTx showed impaired performance, as revealed by a slower time to descend (**Fig. 2f,** left panel). This difference was not observed when mice were pre-treated with the DA synthesis precursor L-DOPA (**Fig. 2f,** right panel), arguing that the motor impairments observed in the adoptively transferred mice were linked to reduced

DA levels. Like for the other behavioral tests, PINK1 KO and WT littermates did not differ, suggesting that a similar neurodegenerative process occurred in both genotypes.

Figure 2

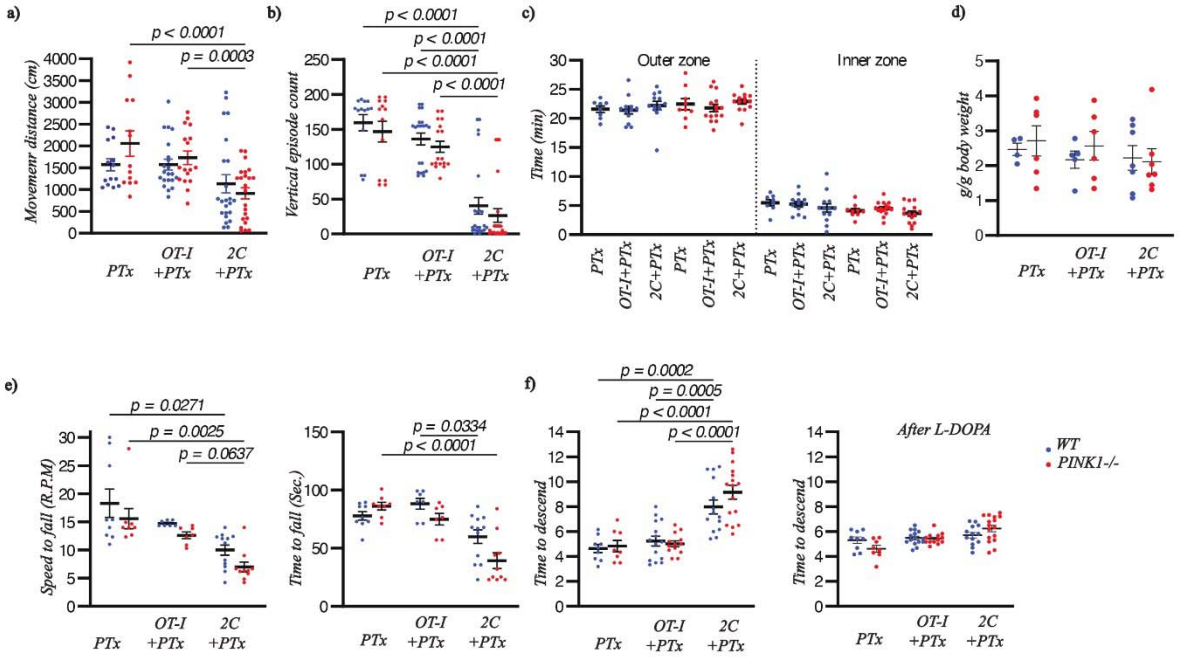

Figure 2: Adoptive transfer of mitochondrial antigen-specific CD8$^+$ T cells leads to L-DOPA reversible motor impairment in both PINK1 KO and WT mice. **a)** In the open field test, the mice were examined for a period of 30min. Total movement distance travelled by mice in an open field arena was measured. **b)** Vertical episodes (number of time that the mouse rears). **c)** Time spent in the outer zone vs inner zone of the open field. **d)** Grip strength for the four limbs normalized by mouse body weight. **e)** Rotarod analysis of the maximal speed and time to fall. **f**) Time to descent in the pole test before (left panel) and 15-30 min after i.p. administration of L-DOPA (25mg/kg) and the dopadecarboxylase inhibitor benserazide (6.5 mg/kg) (right panel). Motor functions were analyzed between days 42 and 56 after the adoptive T cell transfer. Data are representative of four independent experiments for a, b, c, and f and three independent experiments for d and e. *p* values were determined via two-way ANOVA followed by Tukey's multiple comparison's test. Data are presented as mean ± s.e.m. The data combines both male and female mice.

Adoptive transfer of mitochondrial antigen-specific CD8$^+$ T cells causes dopaminergic denervation in the striatum of both PINK1 KO and WT mice.

The motor dysfunctions observed after adoptive transfer of 2C CD8$^+$ T cells could result from perturbations of basal ganglia circuitry, leading to impaired motor commands. Because DA is a critical regulator of basal ganglia circuitry and DA neurons are known to be particularly vulnerable to cellular stress[28], we hypothesized that this system could be negatively affected by mechanisms driven by 2C

322 $CD8^+$ T cells entry in the brain. This hypothesis is also supported by prior *in vitro* work suggesting the
323 capacity of DA neurons to express MHC class I molecules and present antigens to $CD8^+$ T cells[19, 29].
324 Here, we used immunohistochemistry on brain sections prepared from mice 40 days after the adoptive
325 transfer of $CD8^+$ T cells. We find that the dorsal striatum, the main projection area of SNc DA neurons
326 and known to be most affected in PD, of mice that received 2C $CD8^+$ T cells showed a substantial loss
327 of the density of both tyrosine hydroxylase (TH) and DA transporter (DAT) immunoreactivity (**Fig. 3**
328 **and Fig. 4**). No significant changes were observed in mice adoptively transferred with OT-I $CD8^+$ T
329 cells or in mice with only PTx treatment. In the ventral striatum, the same tendency was observed (**Fig.**
330 **4** and **Supplementary Fig. 2**). Decreases in TH and DAT were similar in PINK1 KO and WT mice
331 (**Fig. 4**). We also examined whether this loss of DA neuron axon terminal markers was selective or
332 whether it affected other axonal projections to the striatum or neurons intrinsic to the striatum. For this,
333 we quantified the levels of immunoreactivity for the serotonin (5-HT) axon terminal marker SERT (5-
334 HT transporter) and NeuN, labelling all striatal neuron cell bodies. We found that these signals were not
335 significantly changed (**Figs. 3-4 and Supplementary Fig. 2**). These observations are consistent with the
336 hypothesis that the motor dysfunctions induced by the adoptive transfer of mitochondrial antigen-
337 specific $CD8^+$ T cells and entry of these cells in the brain led to an attack on the DA system.

Figure 3

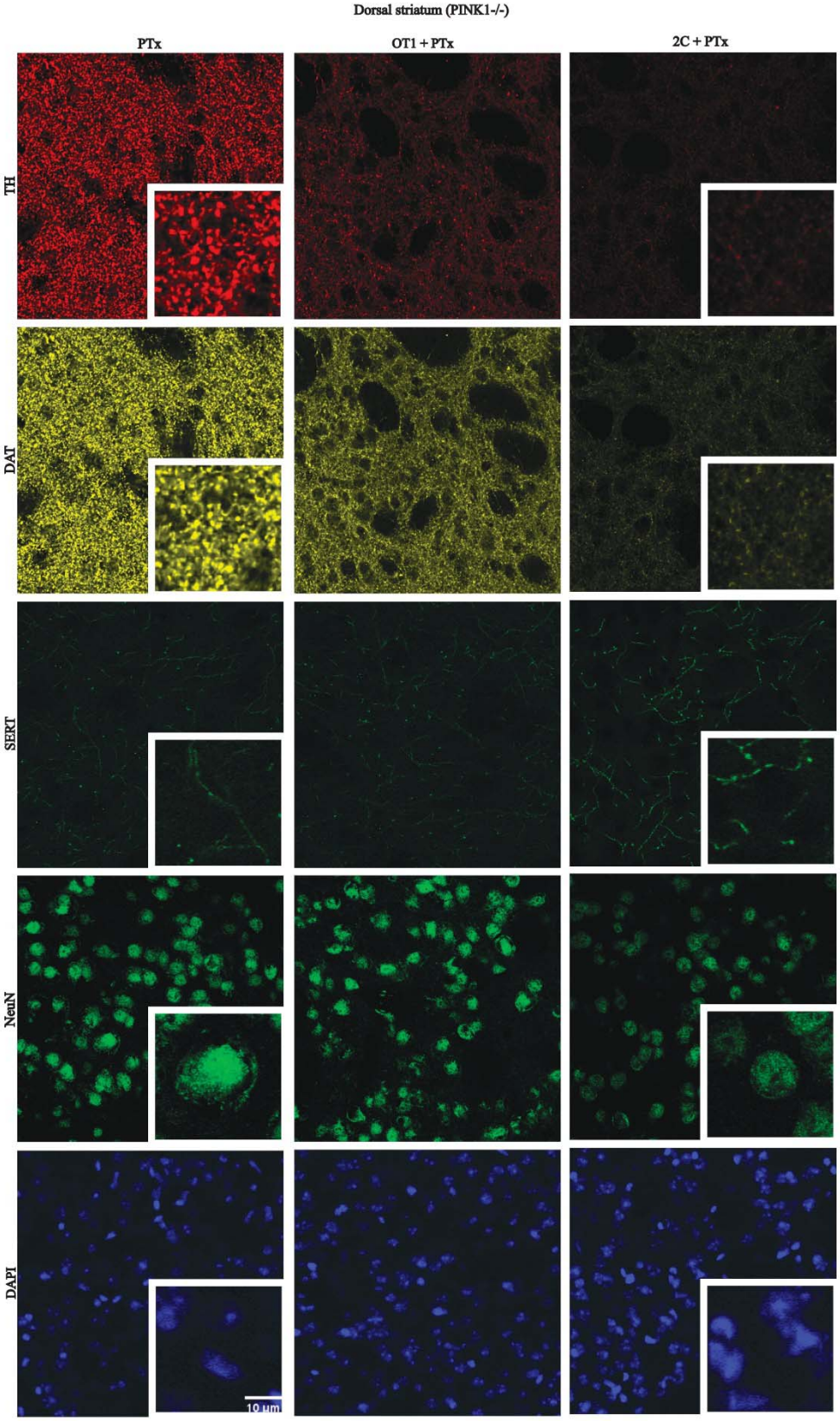

338

Figure 3 : Adoptive transfer of mitochondrial antigen-specific CD8$^+$ T cells causes dopaminergic denervation in the striatum of both PINK1 KO and WT mice. Immunofluorescence staining of the dorsal striatum showing the expression of the dopaminergic neuronal markers tyrosine hydroxylase (TH) (red) and dopamine transporter (DAT) (yellow). The third row of images shows signal for the serotonin (5-HT) membrane transporter (SERT) (dark green). Finally, neuronal nuclei were localized with NeuN (bright green), while total cell population in the tissue was quantified using the nuclear stain DAPI (blue).

Figure 4

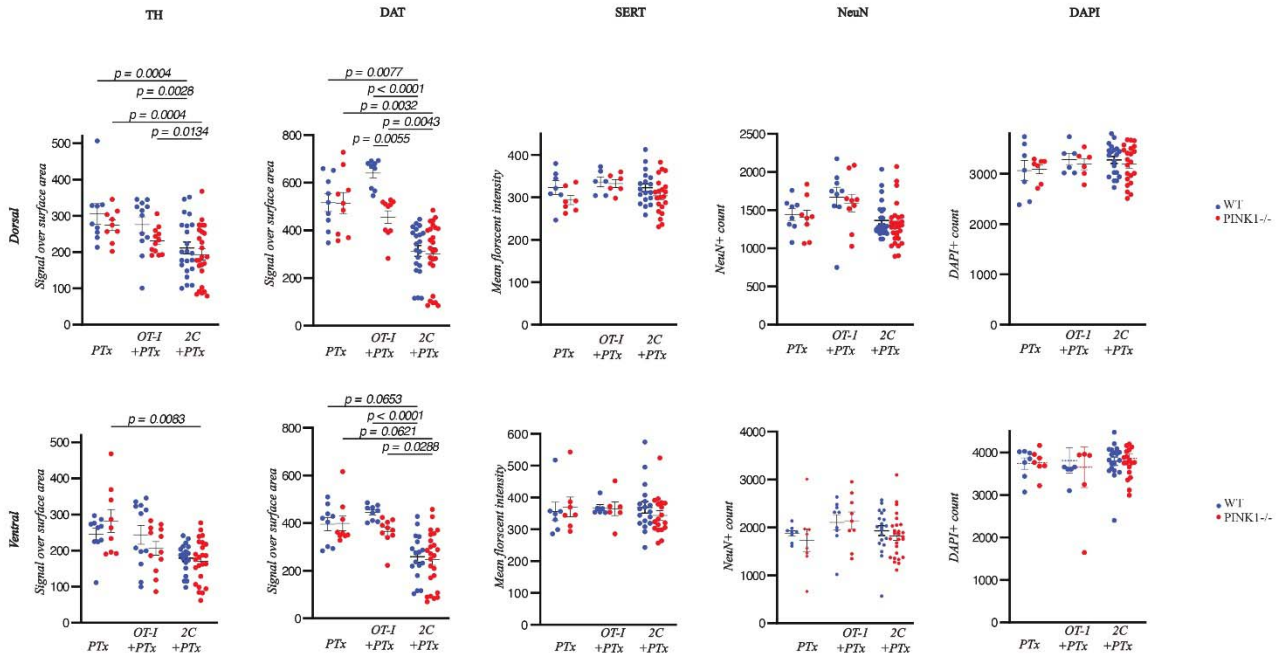

Figure 4: Quantification of the changes in dopaminergic terminal markers reveals that adoptive transfer of mitochondrial antigen-specific CD8$^+$ T cells caused selective dopaminergic denervation in the striatum of both PINK1 KO and WT mice. Quantification of TH, DAT, SERT signal intensity in the dorsal and ventral striatum as determined by signal strength per unit area. NeuN and DAPI represented as absolute count per unit area. Brains were collected at days 42-56 after the adoptive transfer of CD8$^+$ T cells. p value determined using two-way ANOVA, followed by Tukey's multiple comparison's test. Data are presented as mean ± s.e.m.

Adoptive transfer of activated mitochondrial antigen-specific CD8$^+$ T cells leads to degeneration of dopamine neuron cell bodies in the substantia nigra

Loss of axon terminal markers in the striatum could result from a selective attack on axon terminals or from loss of DA neuron cell bodies in the ventral midbrain, including the SNc and VTA. To examine this, we performed a separate series of immunohistochemistry quantification of TH immunoreactive cell bodies in the SNc and VTA using unbiased stereological counting methods. We found that the number

of DA neuron cell bodies was reduced in the SNc but not in the VTA following the adoptive transfer of mitochondrial antigen-specific 2C CD8$^+$ T cells. This was not observed following transfer of the control OT-I CD8$^+$ T cells (**Fig. 5a-b**). The extent of cell body loss was similar for PINK1 KO and WT mice (**Fig. 5b**). Furthermore, no changes in the number of TH-negative neurons were observed (**Fig. 5c**). Altogether, these observations suggest that the loss of terminal markers in the striatum induced by the adoptive transfer of mitochondrial antigen-specific CD8$^+$ T cells is linked to the selective loss of SNc DA neurons in the ventral midbrain.

Figure 5

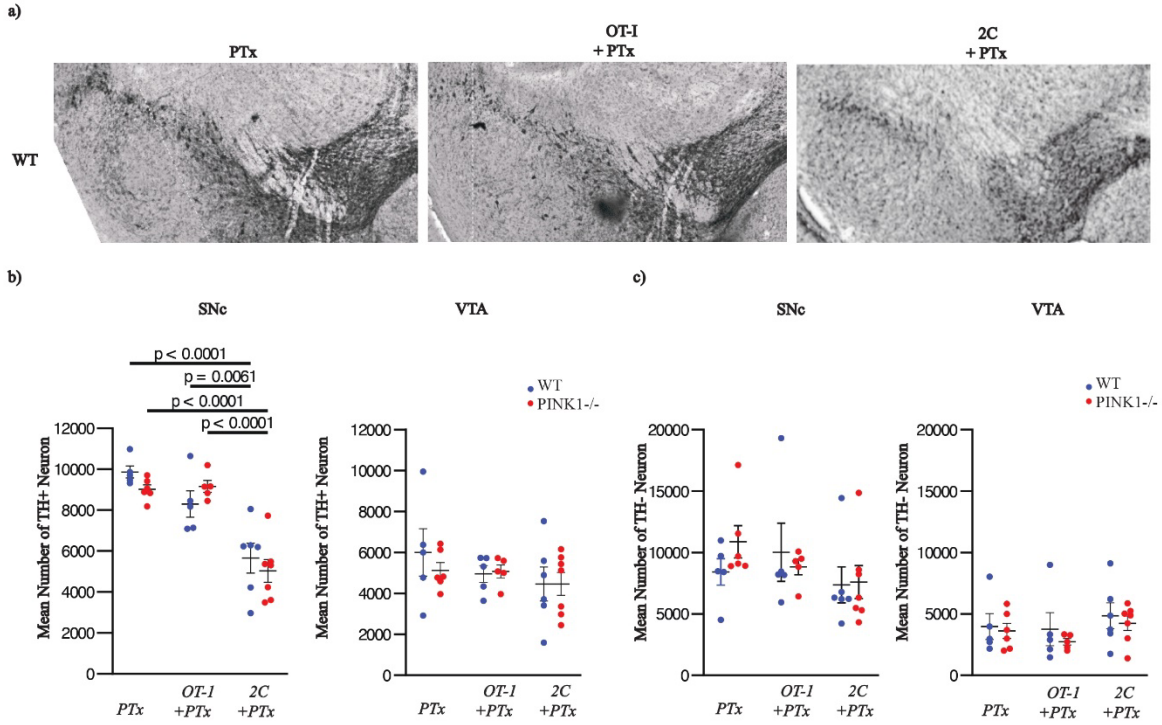

Figure 5: Adoptive transfer of activated mitochondrial antigen-specific CD8$^+$ T cells leads to loss of dopamine neuron cell bodies in the substantia nigra. a) Representative images of the DAB staining used for stereological counting of TH+ dopaminergic neurons in the ventral midbrain. **b-c)** Stereological counting of TH+ and TH- neurons in the ventral tegmental area (VTA) and substantia nigra pars compacta (SNc). Data pooled from three independent experiments. Data are presented as mean ± s.e.m.

Discussion

The mechanisms leading in PD to the loss of DA neurons and other vulnerable neuronal subgroups such as noradrenergic neurons of the locus coeruleus are still ill-defined [28]. However, an increasing amount of evidence suggests that inflammation and immune mechanisms may be involved. A growing series of studies focusing on gene products linked to familial, genetic forms of PD, suggest that multiple PD-related proteins including Parkin, PINK1 and LRRK2 act as regulators of innate and adaptive immune responses in APCs and that loss of function of some of these proteins can amplify immune responses [1, 13-15, 20-23, 30, 31]. Recent work showed that, in inflammatory conditions, PINK1 and Parkin play a role in restricting the presentation on MHC class I molecules of antigens derived from proteins present in the matrix of mitochondria. Indeed, the loss of expression of PINK1 increased MitAP while overexpression of Parkin inhibited this presentation pathway in response to the Gram-negative surface molecule lipopolysaccharide (LPS) in APCs *in vitro* [1]. These data led to the hypothesis that a loss of function of either PINK1 or Parkin results in the presentation of mitochondrial antigens and the stimulation of autoreactive $CD8^+$ T cells that contribute to the pathophysiological process leading to neuronal loss in PD. We have shown that MitAP can be activated following gut infection with Gram-negative bacteria in PINK1 KO mice, a process that leads to the activation of mitochondrial antigen-specific $CD8^+$ T cells and the concomitant development of motor impairments reversible by L-DOPA [19]. Although this chain of events was observed in infected PINK1 KO mice, evidence of a direct role for $CD8^+$ T cells in neuronal loss and the emergence of the motor impairments was not clearly established. Here we extend these previous observations by providing for the most direct test to date of the capacity of mitochondrial antigen-specific activated $CD8^+$ T cells to attack the DA system and cause parkinsonism in mice. Globally, our findings of brain entry and amplification of such $CD8^+$ T cells, loss

of DA neuron axon terminal markers in the striatum, loss of DA neuron cell bodies in the SNc and impaired motor functions support the hypothesis that entry of activated mitochondrial antigen-specific $CD8^+$ T cells in the brain is sufficient to cause neuronal damage and functional impairment.

We found that after adoptive transfer of *in vitro* activated $CD8^+$ T cells specific for either OGDH or ovalbumin, such cells are readily detectable in the periphery and brain of both PINK1 KO and WT mice. However, the abundance of mitochondrial antigen-specific 2C $CD8^+$T cells in recipient mice 40 days after the transfer was higher compared to mice adoptively transferred with ovalbumin-specific $CD8^+$ T cells. This suggests that re-encountering of the antigen by 2C T cells promotes their accumulation and further indicates that the mitochondrial protein OGDH is being presented by MHC class I molecules *in vivo* at steady state in both the presence and absence of PINK1. This contrasts with previous work reporting an enhancement of mitochondrial antigen-presentation only in PINK1 KO mice [19]. This could perhaps result from the fact that previously activated $CD8^+$ T cells have a lower threshold for activation following antigen recognition. Although 2C T cells accumulate more than OT-I T cells, we found increased presence of 2C T cells in the spleen and the brain of PINK KO compared to PINK WT mice. These observations are compatible with the hypothesis that PINK1 deficiency leads to enhanced presentation of mitochondrial antigens as reported previously [1]. Alternatively, PINK1 deficiency could impact other aspects of the $CD8^+$ T cell response such as the cytokine milieu or functions of antigen-presenting cells.

Qualitative examination of the mice after the adoptive T cell transfer suggested the gradual appearance of motor dysfunctions. A more quantitative examination of the mice with a battery of behavioral tasks 42-56 days after the adoptive transfer of $CD8^+$ T cells confirmed the presence of behavioral

impairments, both in the open field, rotarod and in the pole tests. Furthermore, the motor impairments in the pole test were reversed by L-DOPA administration, arguing in favor of the fact that they were caused at least in part by reduced DA levels in the brain. These observations are similar to what was previously observed in PINK1 KO mice after gastrointestinal infection in a previous study [19]. These findings extend the previous study by showing that $CD8^+$ T cells are likely to be a major driver of brain pathology and the appearance of parkinsonism. Further work will be required to determine whether other behaviors linked to non-motor symptoms of PD are also affected in these mice. This could include olfaction, sleep, gastrointestinal functions and cognition.

A surprising finding was that motor impairments developed both in PINK1 WT and KO mice upon T cell adoptive transfer. The fact that PINK1 inhibits the presentation of mitochondrial antigens by APCs suggests that one of the main roles of this protein in the context of PD is to prevent the initiation of the disease process by restricting the stimulation of auto-reactive $CD8^+$ T cells. Accordingly, introducing cytotoxic T cells by adoptive transfer would bypass the protective function of PINK1 and engage a pathophysiological process in both WT and KO mice. This implies that the presence of functional PINK1 proteins in DA neurons cannot prevent the damage to the dopaminergic system and the resulting motor impairments once cytotoxic T cells are elicited.

Our observation of a reduced density of DA neuron axon terminal markers in the striatum of the 2C but not in the OT-I $CD8^+$ T cells transferred mice provides a possible explanation for the L-DOPA-sensitive behavioral impairment observed in the present experiments. Our finding of a lack of change in 5-HT neuron axon terminal marker (SERT) in the same striatal sections argues that the T cell-mediated attack was not non-selective and had a larger impact on the brain's most vulnerable neurons. Our finding of

unaltered number of NeuN-positive neurons or total DAPI-positive cells in these striatal sections also suggests a lack of non-specific neuronal toxicity in these mice. Nonetheless, further examination of markers for other neurotransmitter systems possibly also affected in PD, such as norepinephrine and cholinergic neuromodulatory systems would help extend this conclusion.

The specific mechanisms at play, linking $CD8^+$ T cells entry and DA system dysfunction, remain to be examined. Based on previous work suggesting that DA neurons have the capacity to express MHC class I molecules on their surface [29], one possibility is that in these mice, following the adoptive transfer of 2C $CD8^+$ T cells and PTx treatment, DA neurons present mitochondrial antigens leading to their direct recognition and attack by $CD8^+$ T cells. However, more work is needed to characterize the extent and dynamics of MHC class I expression by DA neurons in both PINK1 KO and WT mice. Our finding of an equivalent attack of DA neurons by activated 2C $CD8^+$ T cells in PINK1 KO and WT mice suggests that such antigen presentation could happen in both genotypes, although not necessarily at the same levels. This raises the hypothesis that in forms of PD linked to loss of PINK1 function, a critical step depends on peripheral mechanisms leading to the amplification of mitochondrial antigen-specific $CD8^+$ T cells. As such, the loss of PINK1 function directly in DA neurons may be less critical. Further work will be required to clarify this. Other than a direct attack of DA neurons by activated $CD8^+$ T cells, another possible mechanism could implicate MitAP by microglia, leading to the secretion of neurotoxic agents by both activated microglia and activated $CD8^+$ T cells. Such mechanisms could rely for example on the secretion of cytokines by $CD8^+$ T cells following recognition of their antigen on microglia, leading to activation of microglia that would then produce inflammatory mediators leading to DA neuron loss. Another possibility is that activated microglia produces ROS that selectively affects the DA

system. A growing literature suggests the implication of similar mechanisms implicating CD8 T cells in Alzheimer's disease [33-36].

Our work provides a different perspective on how PINK1 loss of function could lead to the dysfunction and loss of DA neurons. PINK1 was first shown to be involved in the clearance of damaged mitochondria by mitophagy [33, 37-40]. Such observations were taken by some to imply that loss of PINK1 function in DA neurons would lead to the accumulation of damaged mitochondria in these neurons, eventually promoting their death. However, mitophagy still proceeds in the absence of PINK1 [41-44] and there is presently very limited evidence that dysfunctional mitochondria indeed accumulate in PINK1 or Parkin KO DA neurons [45]. Although we did not directly evaluate the functions of neuronal PINK1 in the present study, our results are more compatible with the hypothesis that loss of function of PINK1 engages autoimmune mechanisms in the periphery at early stages of the disease process. By disinhibiting MitAP and the activation of mitochondria antigen-specific $CD8^+$ T cells, shown here to be responsible for alteration of the dopaminergic system, loss of function of PINK1 may lead to enhanced activation of the immune system in what is likely to be a complex non-cell autonomous process responsible for DA neuron cell death and hallmark motor impairments.

Taken together, our observations provide unprecedented support for a key role of mitochondrial antigen-specific $CD8^+$ T cells in DA system perturbations and associated parkinsonism in mouse models of early-onset PD. This work could be instrumental for the development of better animal models of PD and for the identification of new immune-based therapeutic approaches to treat PD patients.

Acknowledgements

We would like to thank Drs. Michel Desjardins, Samantha Gruenheid, Heidi McBride and Janelle Drouin-Ouellet for their critical feedback during the development of this project. We also thank Dr. Numa Dancause for providing access to their stereological counting microscope system. The present study was funded by the joint efforts of the Michael J. Fox Foundation for Parkinson's Research (MJFF) and the Aligning Science Across Parkinson's (ASAP) initiative. MJFF administers the grant ASAP 000525 on behalf of ASAP and itself. The Trudeau lab also received support from the Canadian Institutes of Health Research (CIHR) (grant 165928) and from the Krembil foundation. M. N. E. received a graduate student award from the mission sector of the ministry of higher education, Egypt.

Author contributions

Conceptualization: N.L., D.M. and L-E.T.
Methodology: M.N.E., J-F.D., A.T., S.B., S.M., N.G., R.H-A, A.E.
Investigation: M.N.E., J-F.D., A.T., S.B., S.M., N.G., R.H-A, A.E.
Supervision: N.L., J.A.S. and L-E.T.
Writing—original draft: M.N.E., N.L. and L-E.T.
Writing—review & editing: M.N.E., N.L. and L-E.T.

Competing interests:

The authors declare that they have no conflicts of interest.

Data and materials availability:

All key data is included in the manuscript. Access to original raw images is available on request from the corresponding authors.

References

1. Matheoud, D., et al., *Parkinson's disease-related proteins PINK1 and Parkin repress mitochondrial antigen presentation.* Cell, 2016. **166**(2): p. 314-327.
2. Drouin-Ouellet, J., et al., *Age-related pathological impairments in directly reprogrammed dopaminergic neurons derived from patients with idiopathic Parkinson's disease.* Stem Cell Reports, 2022. **17**(10): p. 2203-2219.
3. Drouin-Ouellet, J., *Mitochondrial complex I deficiency and Parkinson disease.* Nat Rev Neurosci, 2023. **24**(4): p. 193.
4. Fava, V.M., et al., *Pleiotropic effects for Parkin and LRRK2 in leprosy type-1 reactions and Parkinson's disease.* Proc Natl Acad Sci U S A, 2019. **116**(31): p. 15616-15624.
5. de Leseleuc, L., et al., *PARK2 mediates interleukin 6 and monocyte chemoattractant protein 1 production by human macrophages.* PLoS Negl Trop Dis, 2013. **7**(1): p. e2015.
6. Wallings, R.L., et al., *ASO-mediated knockdown or kinase inhibition of G2019S-Lrrk2 modulates lysosomal tubule-associated antigen presentation in macrophages.* Mol Ther Nucleic Acids, 2023. **34**: p. 102064.
7. Al-Azzawi, Z.A.M., S. Arfaie, and Z. Gan-Or, *GBA1 and The Immune System: A Potential Role in Parkinson's Disease?* J Parkinsons Dis, 2022. **12**(s1): p. S53-S64.
8. Kim, K.S., et al., *Regulation of myeloid cell phagocytosis by LRRK2 via WAVE2 complex stabilization is altered in Parkinson's disease.* Proc Natl Acad Sci U S A, 2018. **115**(22): p. E5164-E5173.
9. Taylor, M. and D.R. Alessi, *Advances in elucidating the function of leucine-rich repeat protein kinase-2 in normal cells and Parkinson's disease.* Curr Opin Cell Biol, 2020. **63**: p. 102-113.
10. Mount, M.P., et al., *Involvement of interferon-γ in microglial-mediated loss of dopaminergic neurons.* Journal of Neuroscience, 2007. **27**(12): p. 3328-3337.
11. Koziorowski, D., et al., *Inflammatory cytokines and NT-proCNP in Parkinson's disease patients.* Cytokine, 2012. **60**(3): p. 762-766.
12. Brochard, V., et al., *scher, J. Callebert, J. Launay, C. Duyckaerts, RA Flavell, EC Hirsch and S. Hunot.* The Journal of Clinical Investigation, 2009. **119**: p. 182-192.
13. Singhania, A., et al., *The TCR repertoire of alpha-synuclein-specific T cells in Parkinson's disease is surprisingly diverse.* Sci Rep, 2021. **11**(1): p. 302.
14. Lindestam Arlehamn, C.S., et al., *alpha-Synuclein-specific T cell reactivity is associated with preclinical and early Parkinson's disease.* Nat Commun, 2020. **11**(1): p. 1875.
15. Sulzer, D., et al., *T cells from patients with Parkinson's disease recognize alpha-synuclein peptides.* Nature, 2017. **546**(7660): p. 656-661.
16. Schonhoff, A.M., et al., *Border-associated macrophages mediate the neuroinflammatory response in an alpha-synuclein model of Parkinson disease.* Nat Commun, 2023. **14**(1): p. 3754.
17. Williams, G.P., et al., *CD4 T cells mediate brain inflammation and neurodegeneration in a mouse model of Parkinson's disease.* Brain, 2021. **144**(7): p. 2047-2059.
18. Tiberi, M., et al., *Systemic inflammation triggers long-lasting neuroinflammation and accelerates neurodegeneration in a rat model of Parkinson's disease overexpressing human alpha-synuclein.* 2024.
19. Matheoud, D., et al., *Intestinal infection triggers Parkinson's disease-like symptoms in Pink1(-/-) mice.* Nature, 2019. **571**(7766): p. 565-569.
20. Hobson, B.D. and D. Sulzer, *Neuronal Presentation of Antigen and Its Possible Role in Parkinson's Disease.* J Parkinsons Dis, 2022. **12**(s1): p. S137-S147.

21. Garretti, F., et al., *T cells, alpha-synuclein and Parkinson disease.* Handb Clin Neurol, 2022. **184**: p. 439-455.
22. Fahmy, A.M., et al., *Mitochondrial antigen presentation: a mechanism linking Parkinson's disease to autoimmunity.* Curr Opin Immunol, 2019. **58**: p. 31-37.
23. Fahmy, A.M., et al., *LRRK2 regulates the activation of the unfolded protein response and antigen presentation in macrophages during inflammation.* bioRxiv, 2023: p. 2023.06. 14.545012.
24. Sha, W.C., et al., *Selective expression of an antigen receptor on CD8-bearing T lymphocytes in transgenic mice.* Nature, 1988. **335**(6187): p. 271-274.
25. Udaka, K., et al., *Self-MHC-restricted peptides recognized by an alloreactive T lymphocyte clone.* Journal of immunology (Baltimore, Md.: 1950), 1996. **157**(2): p. 670-678.
26. Hogquist, K.A., et al., *T cell receptor antagonist peptides induce positive selection.* Cell, 1994. **76**(1): p. 17-27.
27. HJ, G., *The new stereological tools: disector, fractionator, nucleator and point sampled intercepts and their use in pathological research and diagnosis.* Apmis, 1988. **96**: p. 857-881.
28. Giguere, N., S. Burke Nanni, and L.E. Trudeau, *On Cell Loss and Selective Vulnerability of Neuronal Populations in Parkinson's Disease.* Front Neurol, 2018. **9**: p. 455.
29. Cebrian, C., et al., *MHC-I expression renders catecholaminergic neurons susceptible to T-cell-mediated degeneration.* Nat Commun, 2014. **5**: p. 3633.
30. Williams, G.P., et al., *Unaltered T cell responses to common antigens in individuals with Parkinson's disease.* J Neurol Sci, 2023. **444**: p. 120510.
31. Nguyen, M., et al., *Parkinson's genes orchestrate pyroptosis through selective trafficking of mtDNA to leaky lysosomes.* bioRxiv, 2023: p. 2023.09. 11.557213.
32. Recinto, S.J., et al., *Characterizing the diversity of enteric neurons using Dopamine Transporter (DAT)-Cre reporter mice.* bioRxiv, 2023: p. 2023.06. 16.545271.
33. Laurent, C., et al., *Hippocampal T cell infiltration promotes neuroinflammation and cognitive decline in a mouse model of tauopathy.* Brain, 2017. **140**(1): p. 184-200.
34. Chen, X., et al., *Microglia-mediated T cell infiltration drives neurodegeneration in tauopathy.* Nature, 2023. **615**(7953): p. 668-677.
35. Jorfi, M., et al., *Infiltrating CD8(+) T cells exacerbate Alzheimer's disease pathology in a 3D human neuroimmune axis model.* Nat Neurosci, 2023. **26**(9): p. 1489-1504.
36. Su, W., et al., *CXCR6 orchestrates brain CD8(+) T cell residency and limits mouse Alzheimer's disease pathology.* Nat Immunol, 2023. **24**(10): p. 1735-1747.
37. Narendra, D.P., et al., *PINK1 is selectively stabilized on impaired mitochondria to activate Parkin.* PLoS Biol, 2010. **8**(1): p. e1000298.
38. Geisler, S., et al., *PINK1/Parkin-mediated mitophagy is dependent on VDAC1 and p62/SQSTM1.* Nat Cell Biol, 2010. **12**(2): p. 119-31.
39. Kawajiri, S., et al., *PINK1 is recruited to mitochondria with parkin and associates with LC3 in mitophagy.* FEBS Lett, 2010. **584**(6): p. 1073-9.
40. Matsuda, N., et al., *PINK1 stabilized by mitochondrial depolarization recruits Parkin to damaged mitochondria and activates latent Parkin for mitophagy.* J Cell Biol, 2010. **189**(2): p. 211-21.
41. Dagda, R.K., et al., *Loss of PINK1 function promotes mitophagy through effects on oxidative stress and mitochondrial fission.* J Biol Chem, 2009. **284**(20): p. 13843-13855.
42. McWilliams, T.G., et al., *Basal Mitophagy Occurs Independently of PINK1 in Mouse Tissues of High Metabolic Demand.* Cell Metab, 2018. **27**(2): p. 439-449 e5.

608 43. Oshima, Y., et al., *Parkin-independent mitophagy via Drp1-mediated outer membrane severing*
609 *and inner membrane ubiquitination.* J Cell Biol, 2021. **220**(6).
610 44. Miyazaki, N., et al., *PINK1-dependent and Parkin-independent mitophagy is involved in*
611 *reprogramming of glycometabolism in pancreatic cancer cells.* Biochem Biophys Res Commun,
612 2022. **625**: p. 167-173.
613 45. Giguere, N., et al., *Comparative analysis of Parkinson's disease-associated genes in mice reveals*
614 *altered survival and bioenergetics of Parkin-deficient dopamine neurons.* J Biol Chem, 2018.
615 **293**(25): p. 9580-9593.

616